Electronic Supplementary Information

Controlling Interfacial Contact and Exposed Facets for Enhancing Photocatalysis via 2D-2D Heterostructure

Fan Dong[a]*, Ting Xiong[a], Yanjuan Sun[a], Yuxin Zhang[b], Ying Zhou[c]

[a] Chongqing Key Laboratory of Catalysis and Functional Organic Molecules, College of Environmental and Biological Engineering, Chongqing Technology and Business University, Chongqing, 400067, China.

[b] College of Materials Science and Engineering, Chongqing University, Chongqing, 400044, China.

[c] State Key Laboratory of Oil and Gas Reservoir and Exploitation, School of Materials Science and Engineering, Southwest Petroleum University, Chengdu 610500, China.

*To whom the correspondence should be addressed. E-mail: dfctbu@126.com (Fan Dong)

● Experimental Section

1.1 Synthesis of $BiOIO_3$/BiOI heterostructured nanocomposites

All chemicals used in this study were analytical grade and were used without further purification. $BiOIO_3$ was obtained by a simple hydrothermal method. In a typical procedure, 0.485 g of $Bi(NO_3)_3 \cdot 5H_2O$ was added to 70 mL H_2O, and stirred vigorously for 30 min. Then, 0.214 g of KIO_3 was added into the above aqueous and continuously stirred for 10min. The resulted suspension was then hydrothermally treated at 150 ^oC for 6 h. Finally, the $BiOIO_3$ product was collected and dried at 60^oC for 12 h.

$BiOIO_3$/BiOI heterostructured nanocomposites were synthesized by a chemical precipitation method at room temperature. A certain amount of $Bi(NO)_3 \cdot 5H_2O$ was dissolved in 80 mL H_2O containing 9 mL of acetic acid, and 0.48 g of $BiOIO_3$ was added into the above aqueous solution and stirred for 10 min. Then, 30 mL aqueous solution containing stoichiometric amount of KI was added dropwise into the solution and stirred for 2h. After the stirring was completed, the resulted suspension was aged for 2 h. Finally, the resulted products were collected by filtration, washed with water and ethanol for four times and dried at 60 ^oC to obtain the final products. Depending on the molar ratio of $BiOIO_3$ to BiOI (1:0, 6:1, 3:1, 1:1, 0:1), different nanocomposites can be synthesized, respectively.

1.2 Characterization

The crystal phases of the sample were analyzed by X-ray diffraction (XRD) with Cu Kα radiation (model D/max RA, Rigaku Co., Japan). Scanning electron microscopy (SEM; model JSM-6490, JEOL, Japan) was used to characterize the morphology of the obtained products. The morphology and structure of the samples were examined by transmission electron microscopy (TEM; JEM-2010, Japan). Fourier transform infrared (FTIR) spectra were recorded on a Nicolet Nexus spectrometer on samples embedded in KBr pellets. X-ray photoelectron spectroscopy (XPS) with Al Kα X-rays (hm = 1486.6 eV) radiation operated at 150 W (Thermo ESCALAB 250, USA) was used to investigate the surface properties. The UV-vis diffuse-reflectance spectrometry (DRS) spectra were obtained for the dry-pressed disk samples using a Scan UV-vis spectrophotometer (TU-1901, China) equipped with an integrating sphere assembly, using 100% $BaSO_4$ as the reflectance sample. Nitrogen adsorption–desorption isotherms were obtained on a nitrogen adsorption apparatus (ASAP 2020, USA). All the samples were degassed at 120 ^oC prior to measurements. The photocurrent response and electrochemical impedance spectra measurements were performed in three-electrode quartz cells with a 0.1 M Na_2SO_4 electrolyte solution. Platinum wire was used as the counter electrode, and saturated calomel electrodes were used as the reference electrodes. The as-prepared samples film electrodes on ITO served as the working electrode. The photoelectrochemical experiment results were recorded using an electrochemical

system (CHI-660B, China). All the photoelectrochemical measurements are performed under visible light of a 500 W Xe lamp coupling with 420 nm cutoff filters, and the average light power is 45 mW/cm^2.

1.3 Evaluation of photocatalytic activity

The photocatalytic activity was investigated by removal of NO at ppb levels in a continuous flow reactor at ambient temperature. The volume of the rectangular reactor, made of stainless steel and covered with Saint-Glass, was 4.5 L (30 cm × 15 cm × 10 cm). For the visible light photocatalytic activity test, A 150 W commercial tungsten halogen lamp (General Electric) was vertically placed outside the reactor, and a UV cut off filter (420 nm) was adopted to remove UV light in the light beam. The photocatalyst (0.1 g) was coated on a dish with a diameter of 12.0 cm. The coated dish was then pre-treated at 70 ^{o}C to remove the water in the suspension. For each photocatalytic activity test, two sample dishes were used to place in the center of the reactor. The NO gas was acquired from a compressed gas cylinder at a concentration of 100 ppm of NO (N_2 balance) with traceable National Institute of Standards and Technology (NIST) standard. The initial concentration of NO was diluted to about 550 ppb by the air stream supplied by a zero air generator (Thermo Environmental Inc., model 111). The desired relative humidity (RH) level of the NO flow was controlled at 50% by passing the zero air streams through a humidification chamber. The gas streams were premixed completely by a gas blender, and the flow rate was controlled at 3.3 L/min by a mass flow controller. After the adsorption–desorption equilibrium was achieved in the dark, the lamp was turned on. The concentration of NO was continuously measured by a chemiluminescence NO analyzer (Thermo Environmental Instruments Inc., model 42c), which monitors NO, NO_2, and NOx (NOx represents NO + NO_2) with a sampling rate of 0.7 L/min. The removal ratio (η) of NO was calculated as $\eta(\%) = (1- C/C_0) \times 100\%$, where C and C_0 are concentrations of NO in the outlet steam and the feeding stream, respectively.

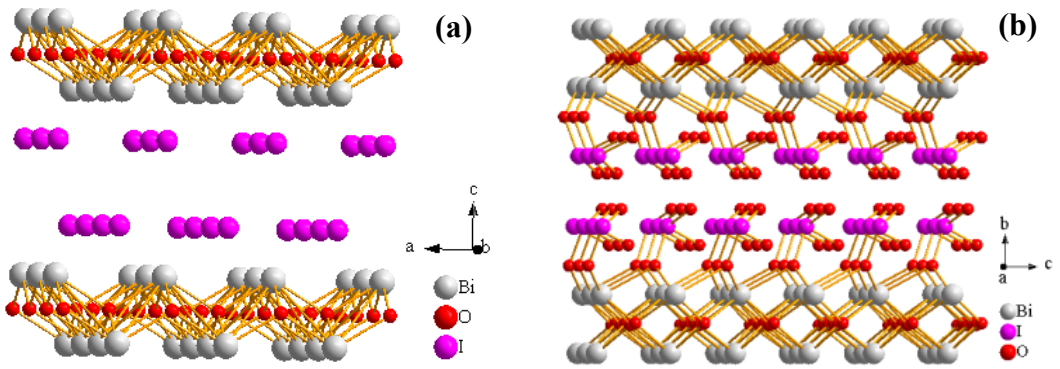

Fig. S1 Crystal structure of BiOI (a) and $BiOIO_3$ (b).

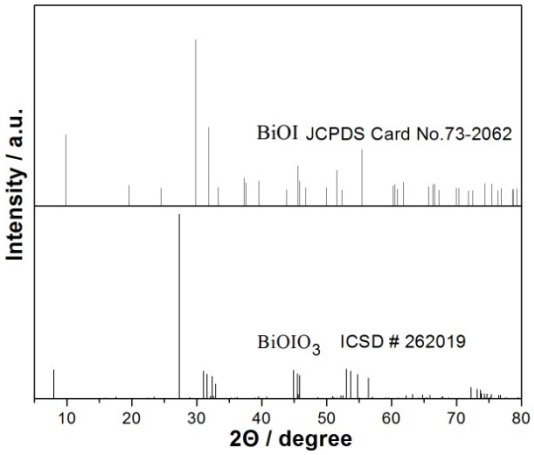

Fig. S2 The standard XRD spectra of the $BiOIO_3$ and BiOI.

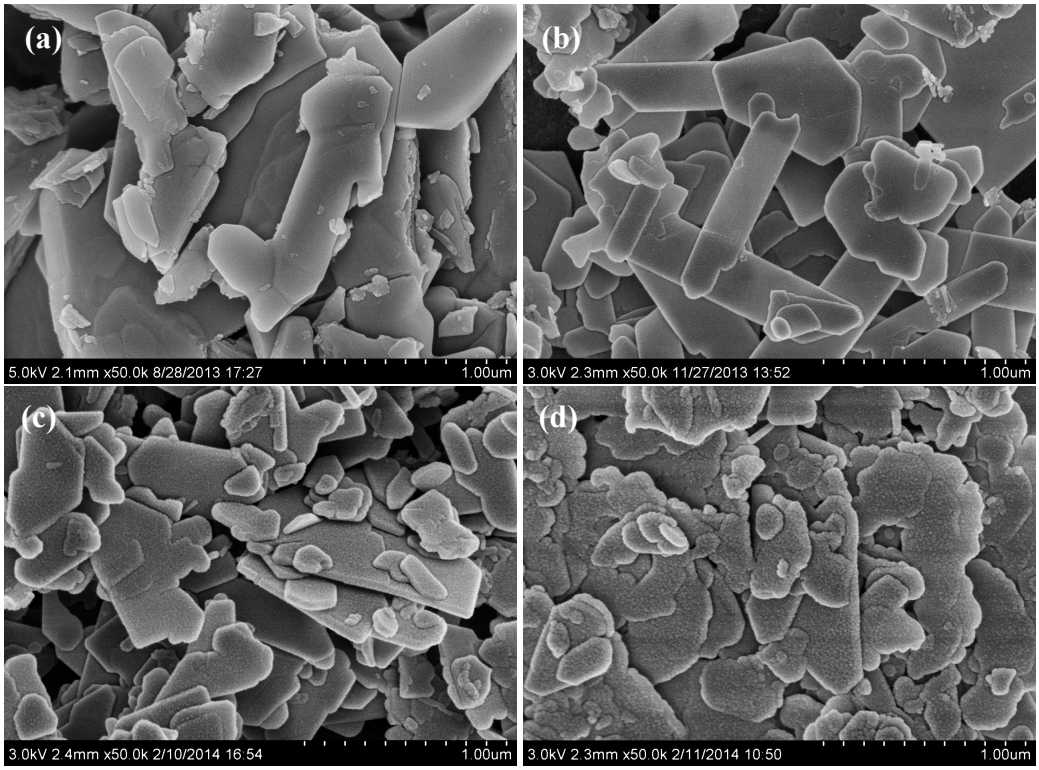

Fig. S3 SEM images of BiOI (a), $BiOIO_3$(b), $BiOIO_3$/BiOI heterostructures with molar ratio of 6:1(c) and 1:1(d).

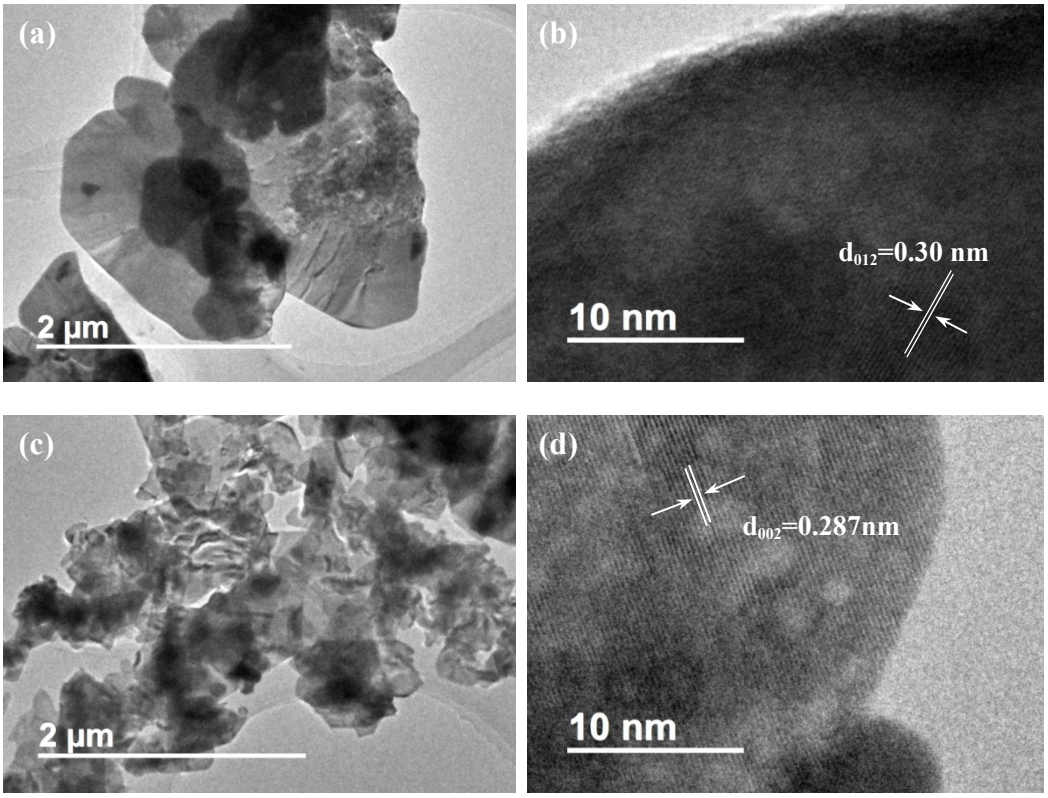

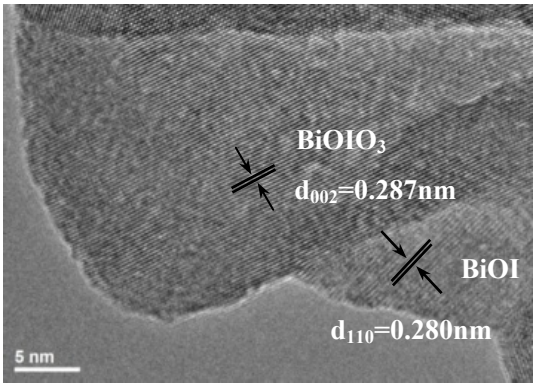

Fig. S4 TEM and HRTEM images of BiOI (a, b) and $BiOIO_3$ (c, d), and the enlarged HRTEM image of the as-prepared $BiOIO_3$/BiOI sample (3:1) (e).

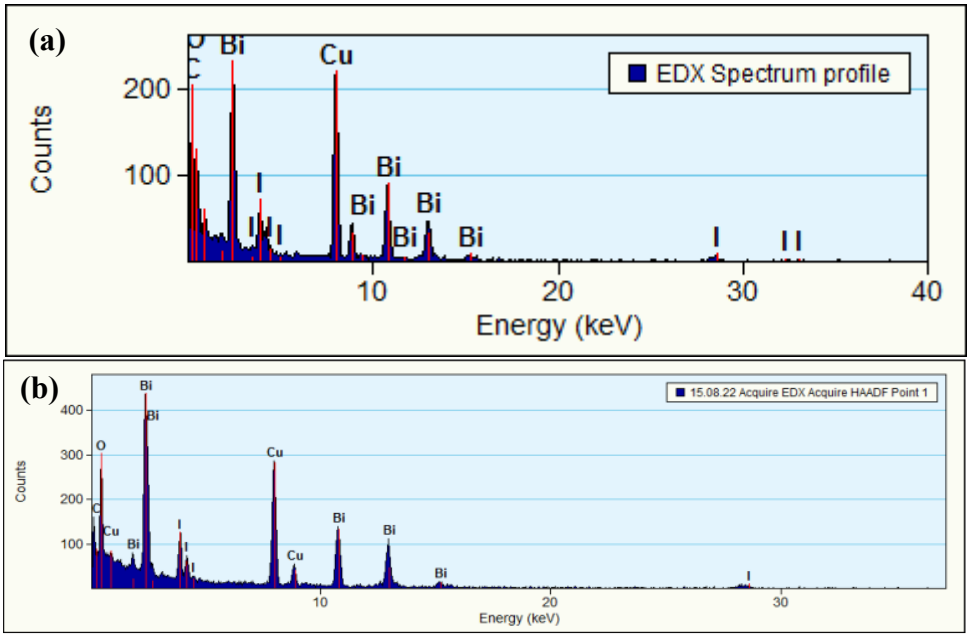

Fig. S5 The EDX line spectra (a) and the EDX point spectra (b) of the as-prepared $BiOIO_3$/BiOI sample (3:1).

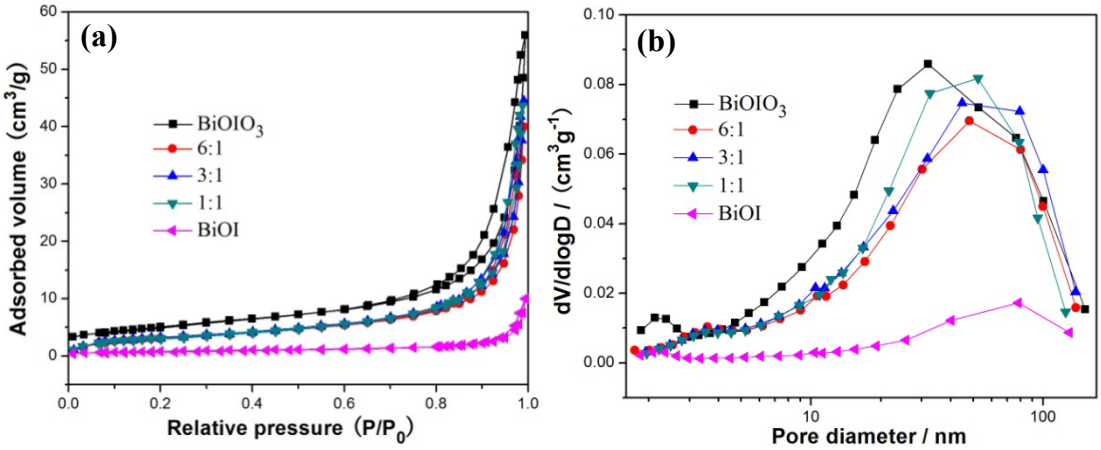

Fig. S6 N_2 adsorption–desorption isotherm (a) and pore-size distribution curve (b) of the as-prepared samples.

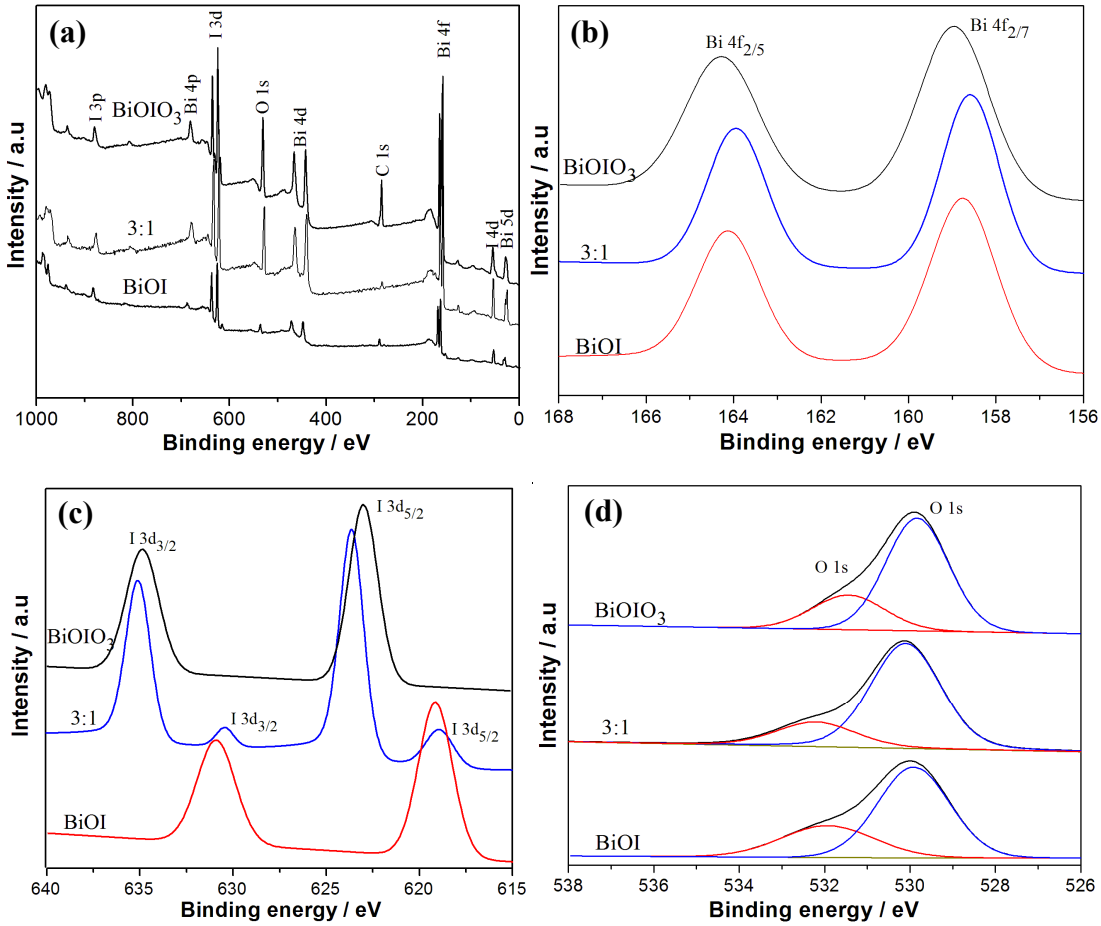

Fig. S7 XPS spectra of $BiOIO_3$, BiOI and the as-prepared $BiOIO_3$/BiOI sample (3:1) : Survey XPS spectrum (a), Bi 4f (b), I 3d (c) and O 1s (d).

The XPS spectra of $BiOIO_3$, BiOI and $BiOIO_3$/BiOI heterostructure (3:1) were further applied to investigate the chemical composition and surface states as shown in Fig. S7. The XPS survey spectra of $BiOIO_3$, BiOI and $BiOIO_3$/BiOI heterostructure (3:1) indicate that the three samples

contain Bi, O, I and some C elements (Fig. S7a). The peak for C 1s (284.8 eV) is attributed to the adventitious carbon. For the $BiOIO_3$/BiOI heterostructure (3:1), two peaks at 164.1 and 158.74 eV are indexed to Bi $4f_{2/5}$ and Bi $4f_{2/7}$, separately, indicating the existence of Bi^{3+} (Fig. S7b). From Fig. S7c, two strong peaks at 635.05 and 623.6 eV are the I $3d_{5/2}$ and I $3d_{3/2}$ states of I^{5+} in $BiOIO_3$, while the other two peaks around 630.4 eV (I $3d_{3/2}$) and 618.9 eV (I $3d_{5/2}$) could be ascribed to the I^- in BiOI.[1-2] In addition, the peaks of O 1s (Fig. S7d) at 530.1 and 532.2 eV corresponding to the Bi-O and I-O bonds and O-H bonds of the surface adsorbed water can be observed. These results further illustrate the coexistence of $BiOIO_3$ and BiOI. Compared with the pure $BiOIO_3$ and BiOI, the binding energies concerning Bi, O and I in $BiOIO_3$/BiOI heterostructure (3:1) all undergo a chemical shift, indicating the strong interaction between $BiOIO_3$ and BiOI benefiting from the intimate contact.

1 L. Ye, L. Tian, T. Peng and L. Zan, *J. Mater. Chem*. 2011, **21**, 12479.

2 W. J. Wang, B. B. Huang, X. C. Ma, Z. Y. Wang, X. Y. Qin, X. Y. Zhang, Y. Dai and M.-H. Whangbo, *Chem. Eur. J.* 2013, **19**, 14777.

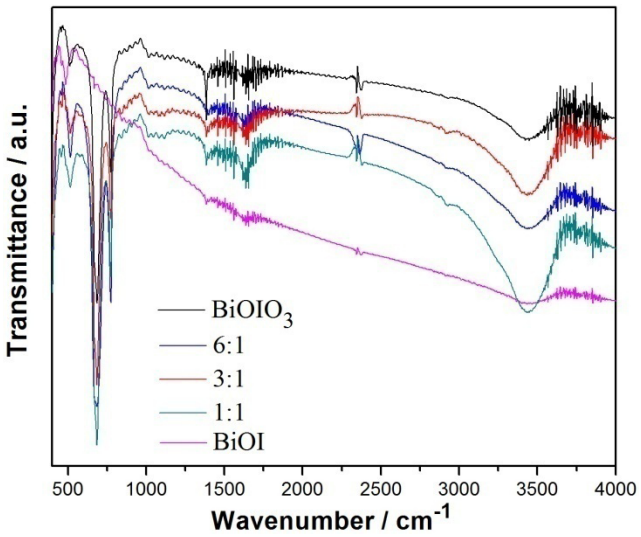

Fig. S8 FT-IR spectra of the as-prepared samples.

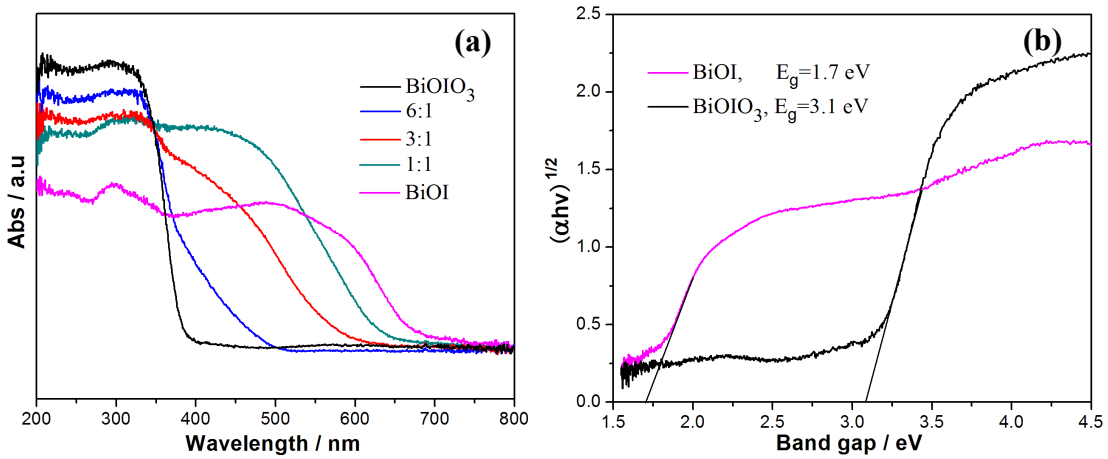

Fig. S9 UV–vis DRS of the as-prepared samples (a) and the plotting of $(\alpha h\nu)^{1/2}$ vs. photon energy of BiOI and $BiOIO_3$ (b).

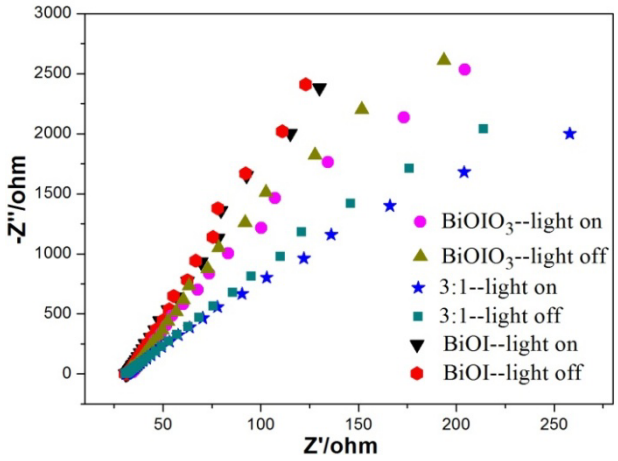

Fig. S10 EIS Nynquist plots of $BiOIO_3$, $BiOIO_3$/BiOI (3:1) and BiOI samples under visible light irradiation ($\lambda > 420$ nm).

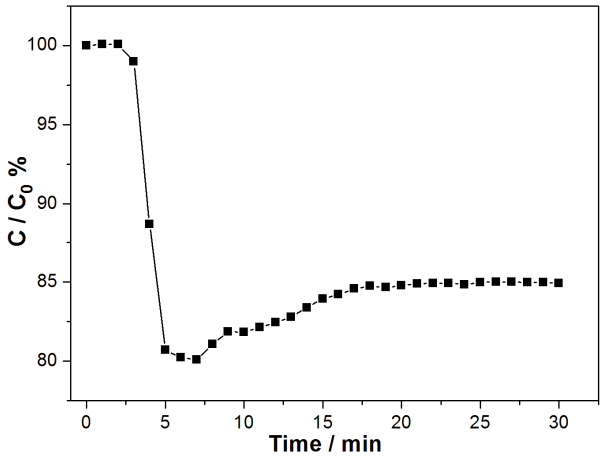

Fig. S11 The photocatalytic performance of the mechanically mixed $BiOIO_3$/BiOI (3:1) sample .